

Article

Evaluation of Mathematical Models for CO₂ Frost Formation in a Cryogenic Moving Bed

David Cann and Carolina Font-Palma * 

School of Engineering, University of Hull, Hull HU6 7RX, UK

* Correspondence: c.font-palma@hull.ac.uk

Abstract: Moving bed heat exchangers (MBHE)s are used in industrial applications including waste heat recovery and the drying of solids. As a result, energy balance models have been developed to simulate the heat transfer between a moving bed and the gas phase. Within these energy balance models, phase change of components within the gas phase has not been considered as the liquefaction or desublimation of the gas phase does not occur in typical industrial applications. However, available energy balance models for cryogenic CO₂ capture (CCC) have only focused on fixed packed beds. The development of a suitable energy balance model to predict the energy duties for MBHEs that include phase change would be beneficial for CCC applications. This work investigated the development of moving bed energy balance models for the design of moving bed columns that involve phase change of CO₂ into frost, using existing models for MBHEs and fixed-bed CCC capture. The models were evaluated by comparison with available moving bed experimental work and simulated data, predicted energy duty requirements and bed flow rates from the suggested moving bed CCC models to maintain thermal equilibrium. The comparisons showed a consistent prediction between the various methods and closely align with the available experimental and simulated data. Comparisons of energy duty and bed flow rate predictions from the developed energy balance models with simulated cases for an oil-fired boiler, combined cycle gas turbine (CCGT) and biogas upgrading showed energy duty requirements for the gas phase with a proximity of 0.1%, 20.8%, and 3.4%, respectively, and comparisons of gas energy duties from developed energy balance models with energy duties derived from experimental results were compared with a proximity of 1.1%, 1.1% and 0.6% to experimental results for CO₂ % v/v concentrations of 18%, 8% and 4%.



Citation: Cann, D.; Font-Palma, C. Evaluation of Mathematical Models for CO₂ Frost Formation in a Cryogenic Moving Bed. *Energies* **2023**, *16*, 2314. <https://doi.org/10.3390/en16052314>

Academic Editor: Artur Blaszczyk

Received: 31 January 2023

Revised: 23 February 2023

Accepted: 24 February 2023

Published: 28 February 2023



Copyright: © 2023 by the authors. Licensee MDPI, Basel, Switzerland. This article is an open access article distributed under the terms and conditions of the Creative Commons Attribution (CC BY) license (<https://creativecommons.org/licenses/by/4.0/>).

Keywords: carbon capture; cryogenic separation; moving bed heat exchanger (MBHE); desublimation

1. Introduction

Anthropogenic emissions of CO₂ to the atmosphere are causing increased global temperatures and climate change. The latest COP27 saw new pledges from governments across the world to reduce emissions and reduce the impacts of climate change [1] including acceleration towards the phase down of unabated coal power and phase-out of inefficient fossil fuel subsidies. Despite its slow scale-up, carbon capture and storage (CCS) is widely regarded as necessary in order to achieve emission reduction targets. CCS is a method of reducing greenhouse gas emissions by capturing CO₂ before it is emitted to the atmosphere and storing it, typically in underground gas reservoirs. Absorption with chemical solvents for carbon capture is the most mature technology currently available; however, this technology has issues scaling down economically to suit smaller-scale applications [2], which opens R&D opportunities for other CCS methods. One option is cryogenic carbon capture (CCC), a CO₂ capture technology that has received growing interest in recent years, and which could suit applications such as biogas upgrading and marine shipping [3]. In addition, it provides advantages over amine-based capture because the process uses physical phase change to separate CO₂ from flue gases because of its relatively high desublimation

temperature. CCC is also able to operate at near-atmospheric pressure when capturing CO₂ as a frost [4].

Cryogenic Carbon Capture Developments

In cryogenic carbon capture (CCC), CO₂ separates out of a flue gas through a physical change due to the high CO₂ desublimation temperature compared with other gaseous components of flue gas. CCC typically utilises a heat exchanger in the form of a packed bed or multiple-plate finned heat exchangers to maximise the heat transfer surface area. As flue gases containing CO₂ desublime out of the gas phase onto the surface of the heat exchangers, the frost forms an insulation layer which reduces heat transfer over time as the temperature driving force for desublimation is reduced as a result of the insulation effect of the frost layer [5]. Maximising the available area of the heat transfer surface increases the available capture time for CO₂ before all available heat transfer surface is saturated with CO₂ frost. Once the available heat transfer area is saturated with frost, the CO₂ capture stops and the heat transfer surface is regenerated in order to recover the CO₂ from the heat transfer surface.

CCC technologies under development include CCC with an external cooling loop (CCC-ECL) [6], anti-sublimation [7] and cryogenic packed beds [8]. Anti-sublimation and cryogenic packed beds operate the heat exchangers in cycles, using multiple heat exchangers in parallel so that one heat exchanger is capturing CO₂ while the other is being regenerated to recover the frost from the heat exchanger surface once it has become saturated with CO₂ frost [9]. CCC-ECL utilises a cryogenic liquid which comes into direct contact with the flue gas to desublime CO₂ within the cryogenic liquid, forming a slurry. The slurry is separated in a later stage to recover the CO₂ and recirculate the cryogenic liquid.

A process utilising a moving bed for CCC is being developed by PMW Technology, known as advanced cryogenic carbon capture (A3C) [10]. The principle is similar to cryogenic packed beds where a cold bed material is used to desublime CO₂ as a frost on the surface of the bed. Whereas a fixed packed bed system would use multiple packed beds operating in cycles of precooling, capture and regeneration stages to create a pseudo-continuous process, a moving bed would remove CO₂ frost saturated bed material from the capture column to regenerate the bed material in a separate sublimator unit, and then recirculate bed material to the capture column. A sketch of the moving bed concept is provided in Figure 1.

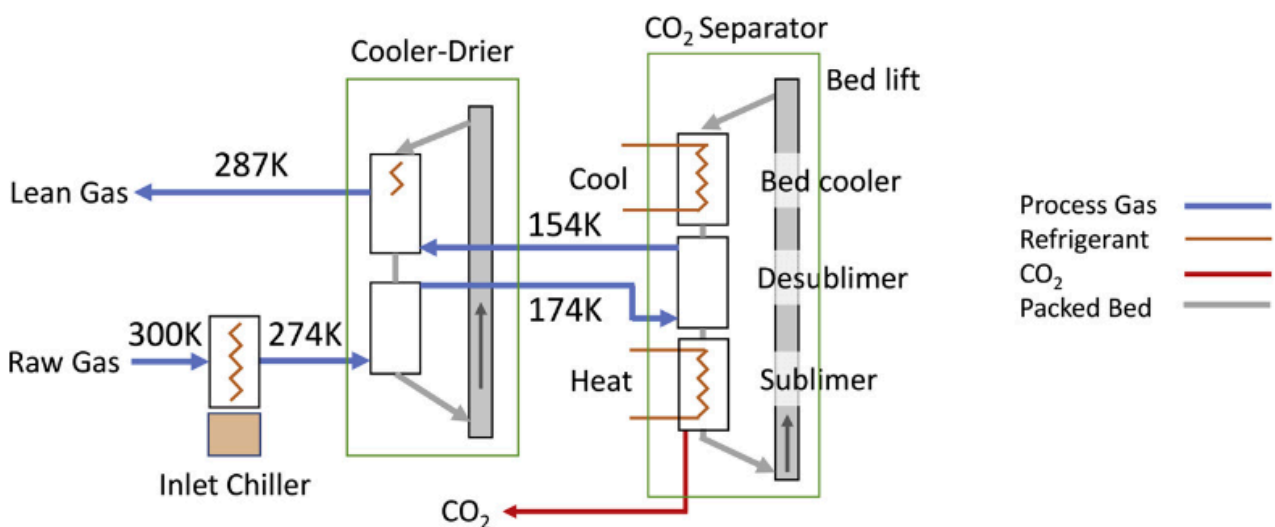


Figure 1. Sketch of the A3C moving bed process [10].

Feasibility studies and experimental demonstrations of the moving bed CCC technology have been performed [10–13]. However, there is a lack of understanding of heat transfer and energy balances in a moving bed, in particular when desublimation of gaseous components are involved as moving bed energy balances do not usually account for phase change. To the best of the authors’ knowledge, current mathematical models for energy balances do not incorporate moving bed flow rates and phase change of components within a packed bed heat exchanger. CCC utilising a moving bed would include extra complexities that current packed bed cryogenic energy balances do not sufficiently account for in regards to bed flow rates and the subsequent effects on temperature profiles within the bed. Whereas, existing moving bed energy balances do not account for phase change and therefore would not accurately predict the behaviour of a cryogenic moving bed as the energy for CO₂ desublimation is a significant energy duty required in the process.

This paper sought to evaluate the effectiveness of available moving bed energy balance equations and identify any modifications needed to account for phase change in the form of desublimation of CO₂. Suitable moving bed heat transfer equations were identified to assess the behaviour of a counter-current moving bed. As the base energy balance equations does not account for the phase change of CO₂ within the energy balance, the expectation is that the energy balance models will be unbalanced between the energy duties of the gas and solid phase in the moving bed heat exchanger by an amount equivalent to the CO₂ desublimation energy requirement. This paper reviewed different methods of modelling CO₂ frost formation on a moving bed using available mathematical models and evaluated the accuracy of these models with empirical data from a purpose-built experimental rig.

2. Mathematical Models for CO₂ Frost

This section reviews current mathematical models; however, they do not fully incorporate the mechanisms for cryogenic CO₂ capture, particularly within a moving bed. They are limited to either mathematical models of frost formation within a static packed bed or heat transfer within a moving bed where phase change does not occur.

2.1. Mathematical Models for CO₂ Frost

Tuinier et al. [8] developed a mathematical model to estimate the CO₂ frost growth within a static packed bed during cryogenic CO₂ capture. They derived Equation (1) for mass balance for the gas phase and (2) for energy balance for the gas and solid phase.

Equation (1) shows how the mass of the gaseous component CO₂ changes across the depth of the packed bed (dz). It also shows how much CO₂ is present in the gas phase on the left-hand side on the equation. The right-hand side of the equation shows how much is desublimated as CO₂ frost as a function of gas velocity, the gas diffusion through the packed bed and CO₂ desublimation rate across the depth of the bed, respectively.

$$\epsilon_g \rho_g \frac{d\omega_{i,g}}{dt} = -\rho_g u_g \frac{d\omega_{i,g}}{dz} + \frac{d}{dz} \left(\rho_g D_{eff} \frac{d\omega_{i,g}}{dz} \right) - \dot{m}_i'' a_s + \omega_{i,g} \sum_{i=1}^{n_c} \dot{m}_i'' a_s \quad (1)$$

Equation (2) represents the available energy duty within the packed bed column on the left-hand side, including the gas filling the void spaces and the total of the solid bed material. The cooling duty required by the gas to desublime CO₂ is presented on the right-hand side of the equation, with terms representing the movement of the gas through the bed, the change in thermal conductivity across the depth of the bed and the desublimation rate of CO₂ out of the gas phase.

$$(\epsilon_g \rho_g c_{p,g} + \rho_s (1 - \epsilon_g) c_{p,s}) \frac{dT}{dt} = -\rho_g u_g c_{p,g} \frac{dT}{dz} + \frac{dT}{dz} \left(\lambda_{eff} \frac{dT}{dz} \right) - \sum_{i=1}^{n_c} \dot{m}_i'' a_s \Delta h_i \quad (2)$$

Both the energy and mass balance include terms for the desublimation of CO₂. Given the energy balance is based on a fixed moving bed, temperature gradients are considered to change over time as the CO₂ frost front advances through the packed bed. Adjusting the

balances to simulate a moving bed, the complexity of the balances due to simulation of a batch process is avoided and changing conditions over time would be substituted for consistent temperature gradients. This eliminates the complexity of variation of temperature gradients when assuming thermal equilibrium.

2.2. Mathematical Models for Moving Bed Heat Exchangers

Moving bed heat exchangers (MBHE) are used to balance heat transfer between the moving bed material and gas stream to provide cooling or heating duty to the solid phase. The gas stream can be either counter-current, co-current or cross flow to the flow of bed material. These flow methods are used in different industrial applications such as waste heat recovery in metallurgical industries [14] or solids drying [15]. Moving beds have also been investigated for the purpose of heat exchange and filtration of solid particulates from a gas [16,17]. Counter current moving bed models would be considered the most suitable energy balance models for the CCC system, while co-current models are the least effective for predictions of the CCC system.

Energy balance models for heat exchangers will generally follow the fundamental principle that energy will transfer between the solid and gas phase (Equation (5)) and that the energy duty will be equivalent based on the mass, specific heat capacity and temperature change of the solid and gas phases, respectively.

$$Q_s = \dot{m}_s c_{p,s} dT_s \tag{3}$$

$$Q_g = \dot{m}_g c_{p,g} dT_g \tag{4}$$

$$Q_s = Q_g \tag{5}$$

It is important to note in Equations (3) and (4) that the temperature change of the gas is typically from initial gas temperature to initial bed temperature as a result of the high heat transfer coefficient, whereas the bed temperature change is from the initial bed temperature to the CO₂ desublimation temperature.

The governing equations for heat transfer in a cross-flow arrangement are provided by Equations (6)–(8) [18].

$$\epsilon \rho_g c_{p,g} (dT_g dt + u_g \cdot \nabla T_g) = \nabla \cdot (k_g \nabla T_g) + h_s a_s (T_s - T_g) \tag{6}$$

$$(1 - \epsilon) \rho_s c_{p,s} (dT_s dt + u_s \cdot \nabla T_s) = \nabla \cdot (k_s \nabla T_s) + h_s a_s (T_g - T_s) \tag{7}$$

$$\dot{m}_s c_{p,s} = LB(1 - \epsilon) \rho_s u_s c_{p,s} = \dot{m}_g c_{p,g} = HB \epsilon \rho_g u_g c_{p,g} \tag{8}$$

Equation (6) balances the mass flow rates and specific heat capacities of the solid bed flow rate and the gas. For this energy balance equation, it may be assumed that the temperature change for the solid and gas phases are equivalent or that the thermal approach temperature is negligible across the heat exchanger. The energy balance is also based on mass flow rates calculated by the cross-sectional area of the heat exchanger and the volume occupied by either the solid or gas phase.

Adapting this energy balance to fit the set up described for the cryogenic moving bed process requires an addition of a term on the gas side of the energy balance to account for CO₂ desublimation. Furthermore, the volume-based energy balance would require adaptation of geometry for the moving bed heat exchanger to better reflect the heat transfer within the cryogenic moving bed.

Governing equations for heat transfer in a counter-current arrangement are provided by Equations (9)–(11) [19].

$$\dot{m}_s c_{p,s} dT_s - h_{g,s} a A_b dH (T_s - T_g) \approx 0 \tag{9}$$

$$\dot{m}_g c_{p,g} dT_g = h_{g,s} a A_b dH (T_s - T_g) - dQ_w \tag{10}$$

where,

$$dQ_w = h_{g,w} S_b dH (T_s - T_g) \quad (11)$$

where dH represents the infinitesimal bed depth. The energy balance equation visualizes what volume of bed material is required to complete heat transfer from the gas phase to the solid bed based on the infinitesimal bed depth. The purpose of developing an energy balance model for the cryogenic moving bed is to understand the required mass flow rate of bed material to balance an incoming flue gas. Assumptions for the infinitesimal bed depth can be applied to simulate the energy balance model for the cryogenic moving bed process.

The proposed energy balance models require a method of validation to demonstrate that the equations can accurately simulate a cryogenic moving bed and provide confidence in the results generated. Feasibility studies of cryogenic moving beds found in the literature were used to test these energy equations [10].

3. Methodology

Mathematical modelling has previously shown that frost front velocities can be accurately predicted for fixed packed beds [11], where the frost front velocity is predicted based on energy duties of the gas and solid phase in a fixed bed. Energy balance equations can be used to predict the behaviour of the fixed bed by calculating the available required energy duty of the gas phase, including the desublimation energy duty. The total energy duty required by the gas phase can be used to evaluate the accuracy of the adjusted energy balance models proposed by this study.

Adjusting Equations (3)–(5) into a moving bed case by calculating the energy balance around a mass flow rate of bed material and gas as opposed to a fixed mass of bed present in the column, the energy balance can make predictions for a moving bed based on the inlet gas flow conditions of the experimental rig.

When desublimation of CO_2 within the gas phase occurs, the latent enthalpy of desublimation will need to be included in Equation (4) for the gas side energy balance to be complete:

$$Q_g = \dot{m}_g c_{p,g} dT_g + \Delta h \omega_{\text{CO}_2} \quad (12)$$

The energy balance model [18] provided in Equation (8) is updated to include a term to represent the desublimation of CO_2 in the moving bed as Equation (13). This balance model will subsequently be referred to as the mass flow balance model.

$$\dot{m}_s c_{p,s} = \dot{m}_g c_{p,g} + \frac{\Delta h \omega_{\text{CO}_2}}{dT} \quad (13)$$

The energy balance model [19] provided in Equation (11) is updated with a term to represent the desublimation of CO_2 within the moving bed. This balance model will be subsequently be referred to as the minimum bed depth model (Equation (14)).

$$\dot{m}_g c_{p,g} dT_g + \Delta h \omega_{\text{CO}_2} = h_{g,s} a A_b dH (T_s - T_g) - dQ_w \quad (14)$$

These energy balance models were utilised by introducing known values such as initial and final temperatures and mass flow rates, from the experimental or simulated data, to produce simulated results to compare with each experimental or simulated data set. For each of the energy balances, temperatures and gas flow rates are available data taken from experimental results in [11] and simulated results in [10]. Other variables such as gas density and heat transfer coefficients are calculated from REFPROP. These results are provided in Appendix A.

In Equation (14), the infinitesimal bed depth is an unknown value that cannot be derived from available information and would therefore be calculated iteratively under the understanding that the equation will balance.

Equation (15) is the heat transfer coefficient calculation for the minimum bed depth model [19], and Equation (16) is an alternative method for calculating the heat transfer coefficient using bed surface area [20]. In Equation (16), the solid phase energy duty is used to represent the total energy duty of the gas phase and the CO₂ desublimation enthalpy; the bed area is calculated based on the cross-sectional area of the capture column and the infinitesimal bed depth that was iteratively found to balance the minimum bed depth model equation. These heat transfer coefficients were calculated and compared to evaluate the validity of the derived infinitesimal bed depth.

$$h_{g,s} = 0.015 \frac{k_g}{d_p} Re^{1.3} \quad (15)$$

$$h_{g,s} = \frac{Q_s}{A_b dT} \quad (16)$$

Figure 2 shows a sketch of the demonstration rig. The demonstration rig was described in [12] and consists of a PTFE pipe with 76 mm internal diameter and 5 mm wall thickness. The capture column was fitted with a copper pipe gas injector 25 mm in diameter which fed a cooling gas of N₂ (blue) and mixed gas of CO₂ and N₂ (orange), and shown in Figure 2. The flow rate and CO₂ concentration in the mixed gas line was measured and controlled using inline rotameters with a precision of 10 LPM, flow control valves and a GSS ExplorIR[®]-W CO₂ sensor which records concentration with a precision of 0.001%. Type-K thermocouples measure the temperature of the mixed gas feed stream and temperatures of the capture column at various bed depths to record the movement of the CO₂ frost front via temperature change. The thermocouples were attached to dataloggers (TC-Direct 4 channel) to record temperature change over time with a precision of 0.1 °C. The N₂ precooling gas was cooled down using a liquid nitrogen bath and used to precool steel bed material with diameters ranging between 1.4 and 1.7 mm and featuring a measured bed voidage of 0.42, with a heat exchanger in place to recover cooling duty from liquid nitrogen boiloff. The steel bed material was precooled down to a temperature of −120 °C, after which the gas stream would be switched the orange mixed gas line. The mixed gas would be cooled to −90 °C through the liquid nitrogen bath and would then be cooled by the bed material sufficiently to desublime CO₂ as a frost on the surface of the bed material. Thermocouples measured over time increased the temperature of the bed material until it reached an equilibrium temperature equivalent to the CO₂ desublimation temperature, when the temperature plateaus. The time taken to reach the temperature plateau advancing through the column was used to calculate a frost front velocity. Frost front velocities were taken as an average of the time taken for the frost front to advance, which could range from ±5 s to ±50 s depending on gas flow rate, CO₂ concentration and distance of the thermocouple to the gas injection point.

Mixed gas compositions were tested experimentally with varying flow rates and CO₂ gas concentrations. Firstly for the purpose of testing the effectiveness of the energy balance models, the varying CO₂ concentration data in Table 1 were used to simulate a moving bed scenario from available fixed packed bed experimental results [11].

Table 1. Inlet flue gas flow rate conditions for cryogenic rig simulation.

Inlet Gas Flow Rate (LPM)	Superficial Velocity (m/s)	Inlet Gas CO ₂ Concentration (% v/v)
100	0.23	18
100	0.23	8
100	0.23	4

The frost front velocity equation in [11] can be rearranged to calculate the energy duty required by the gas; this equation is shown in Equation (17). Calculating this energy

duty allows comparison of energy duties between the proposed energy balances and experimental results from the rig.

$$Q_g = AU_{frost}\rho_s c_{p,s} dT_g \quad (17)$$

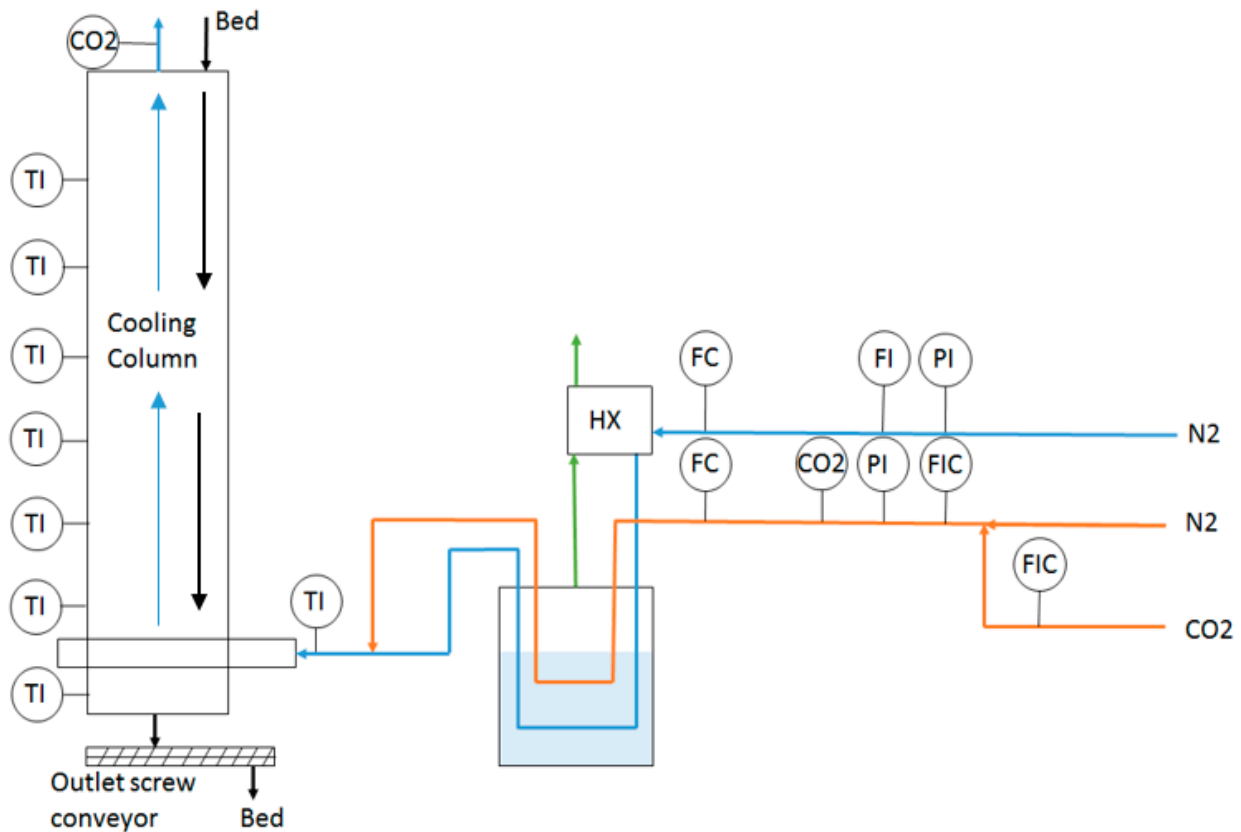


Figure 2. Sketch diagram of the experimental rig [11]. TI, temperature indicator (type K thermocouple), CO₂, GSS ExplorIR[®]-W CO₂ sensor, HX, heat exchanger, FC, flow controller (on/off valve), FIC, flow indicator and controller (rotameter and flow control valve), PI, pressure indicator (pressure gauge).

Secondly, the validity of the energy balance equations was assessed for larger scale CCC moving bed technology. Simulated data from [10] were used to assess the A3C technology for three different industrial applications: an oil-fired boiler, a combined cycle gas turbine (CCGT) and a biogas upgrading process. These flue gases have a defined flow rate and composition, while volumetric bed flow rates were calculated for each of the applications to maintain a continuous process. The bed flow rates were calculated by Willson et al. [10] as 0.55, 0.19 and 0.002 m³/s for the oil-fired boiler, CCGT and biogas upgrading applications, respectively. This work compared the moving bed flow rate and energy duties for various unit operations of the A3C technology reported in [10] using Equations (12)–(14). Demonstrating the validity of the energy balance models for each of these applications would show the robustness of the energy balances to predict the behaviour of moving bed CCC applications of different scales and flue gas conditions.

This work sought to use energy balance models to simulate the desublimer stage of the A3C process in Figure 1. This stage cools down the precooled flue gas from 174 K to 154 K, which would sufficiently cool it to desublime CO₂ present in the flue gas to form a frost on the surface of the moving bed material. Since the energy balance models focus around the desublimer, the A3C process is expected to have removed water in the cooler–drier step. Thus, the flow rates and compositions in [10] were updated and are shown in Table 2 to show dry conditions.

Table 2. Dry gas flow rates and compositions of three applications.

	Oil-Fired Boiler	CCGT	Biogas Upgrading
Gas flow (t/h)	541	458	0.83
CO ₂ % (v/v)	13.79	3.48	35
N ₂ % (v/v)	86.21	81.63	0
O ₂ % (v/v)	0	14.89	0
CH ₄ % (v/v)	0	0	65

This study evaluated the effectiveness of using the available moving bed energy balance models to calculate the energy duty of the desublimer and the required bed flow rate to maintain thermal equilibrium. For the energy balance models, additional terms must be included to satisfy the need for an estimation of the required latent enthalpy of desublimation for CO₂. The latent enthalpy of CO₂ and CO₂ concentration within the flue gas were used to calculate the energy duty for the CO₂ to desublime.

4. Results and Discussion

4.1. Experimental Rig Simulation

Equation (12), as well as the mass flow balance model and minimum bed depth model were used to simulate the experimental cryogenic carbon capture rig and assess the similarity of different energy balance equations for the simulation of the moving bed process.

The energy balance model in Equation (12) was used to estimate the required cooling duty of the gas flows described in [11] for mixed gases containing 18%, 8% and 4% CO₂ in Table 1 cooled from the initial bed temperature (−120 °C) to the initial gas temperature (−90 °C). Equation (12) requires the mass flow rate and specific heat capacity of the gas, which is estimated from the composition of CO₂ and N₂ in the gas phase based on their pure values. The CO₂ desublimation duty was calculated by the latent enthalpy of desublimation and the mass concentration of CO₂ in the gas phase. The total cooling duty required by the gas is the sum of the cooling gas duty and the desublimation duty. The bed energy duty is the sum of these two calculated energy duties to balance Equation (5). Bed flow rate was calculated through Equation (3) to match the energy duty required by the gas phase accordingly. Table 3 shows the results for the cooling gas duty, CO₂ desublimation duty, total bed energy duty and mass flow rate of the bed material. The energy duties and bed flow rates in Table 3 are later compared with experimental results in Table 4 to assess the consistency of the simulated values from Equation (12) with experimental data.

Table 3. Simulated moving bed energy duties and bed flow rates for various CO₂ concentrations using Equation (12).

CO ₂ % v/v	Cooling Duty Gas (W)	CO ₂ Desublimation Duty (W)	Bed Energy Duty (W)	Bed Mass Flow Rate (kg/s)
18	105	335	440	0.026
8	103	149	252	0.018
4	103	75	177	0.014

Table 4. Calculated energy duties from experimental results [11].

CO ₂ % v/v	Frost Front Velocity (mm/s)	Calculated Bed Energy Duty (W)	Error (W)
18	0.784	429	±39
8	0.576	265	±16
4	0.460	182	±6

The energy balance results in Table 3 were verified using experimental results from [11]. The frost front velocities determined experimentally were used to calculate the energy duty of the gas phase shown in Table 4 using Equation (17). The effectiveness of this energy balance model can be evaluated by comparing the accuracy of the bed energy duties in Table 3 with that experimentally derived, as shown in Table 4.

The bed energy duty calculated from the energy balance model closely aligns with the experimental results. The calculated bed energy duties were within 5% of the energy duties derived from the experimental results. Given the error in experimental calculation of the frost front velocity due to time discrepancies, the calculated energy duties from Table 3 would fall within the range of error in the energy duties derived from experimental results shown in Table 4. This provides confidence that the calculated energy duties and bed flow rates in a moving bed case using the energy balance model are justifiable and can be used to evaluate the accuracy of the minimum bed depth model and the mass flow balance model.

The mass flow balance model estimates the mass flow rate of bed material based on the known mass flow rate of the gas phase and specific heat capacities of the bed and gas phases in the moving bed. For the mass flow balance model, the CO₂ desublimation duty was calculated with the same method as above. Table 5 shows the bed mass flow rates and energy duties using the mass flow balance model (Equation (13)).

Table 5. Simulated moving bed energy duties and bed flow rate for various CO₂ concentrations using the mass flow balance model (Equation (13)).

CO ₂ % (v/v)	Gas Mass Flow Rate (kg/s)	Bed Mass Flow Rate (kg/s)	Gas Cooling Duty (W)	Total Cooling Duty (W)
18%	0.0023	0.023	105	440
8%	0.0021	0.013	103	252
4%	0.0021	0.009	103	177

The cooling duty required by the gas phase calculated by the mass flow balance model is equivalent to the energy balance calculated through Equation (12) in Table 3. However, the calculated bed mass flow rates using the mass flow balance model are slightly lower compared with Equation (12). The elimination of temperature change from the energy balance model is the cause for this discrepancy between results.

The mass flow balance model assumes that temperature change for the gas and solid phase are both equal and that the temperature approach of the heat exchanger is negligible. This cannot be considered the case, as CO₂ desublimation occurs. Temperature change of the bed phase is limited to rise from the initial bed temperature to the CO₂ desublimation temperature as opposed to the initial gas temperature. This causes the bed flow rate calculated through the mass balance model to be lower than other calculated values in Table 3. In order to easily compare the calculated bed flow rates and energy duties of the different models, Table 5 shows that the bed, gas cooling and CO₂ desublimation duties were converted to Watts. This was achieved by multiplying each term in Equation (13) by temperature change dT . The bed duty, bed flow rates and total cooling duties in Tables 3 and 5 showed a remarkable similarity between the two mathematical models.

The mass flow rate of the gas was relatively similar for each different case, and the change in required energy duty was predominantly related to the changing CO₂ concentration in the mixed gas. The CO₂ desublimation duty within the energy balance was reduced as the concentration was reduced. The mass flow balance model provided a slightly different bed flow rate than using Equation (12) due to the discrepancy between the temperature change of the solid and gas phases. The mass flow balance would show much closer agreement with other bed flow rate predictions from energy balance models when temperature change between the gas and solid phases are equivalent.

In order to account for changes in CO₂ desublimation temperature with respect to CO₂ concentration v/v , the mass flow energy balance model needs to be modified. Equation (13)

was updated to account for the difference in temperature changes for the gas and solid bed material and shown as follows:

$$\dot{m}_s c_{p,s} dT_s = \left(\dot{m}_g c_{p,g} + \frac{\Delta h \omega_{CO_2}}{dT_g} \right) dT_g \quad (18)$$

This rearrangement is equivalent to Equation (12), since Equation (13) would only be feasible in situations where the temperature difference between the gas phase and solid phase is equivalent. The results of this updated mass flow balance model (Equation (18)) are provided in Table 6.

Table 6. Simulated moving bed energy duties and bed flow rate for various CO₂ concentrations using updated mass flow balance model (Equation (18)).

CO ₂ % (v/v)	Gas Mass Flow Rate (kg/s)	Bed Mass Flow Rate (kg/s)	Gas Cooling Duty (W)	Total Cooling Duty (W)
18%	0.0023	0.026	105	440
8%	0.0021	0.018	103	252
4%	0.0021	0.014	103	177

Equation (14) was balanced using the desublimation energy requirement. With the infinitesimal bed depth not certain, the energy balance was set up to balance the equation by assuming the infinitesimal bed depth to balance the equation. Table 7 provides results from the minimum bed depth energy balance model.

Table 7. Simulated moving bed energy duties and bed flow rate for various CO₂ concentrations using Equation (14).

CO ₂ % (v/v)	Gas Cooling Duty (W)	CO ₂ Desublimation Duty (W)	Wall Losses (W)	Bed Duty (W)	Bed Flow Rate (kg/s)
18%	105	335	5	445	0.026
8%	103	149	3	255	0.018
4%	103	75	3	176	0.014

The energy balances from Equation (14) produced similar energy duties to Equation (6), with minor differences being due to the inclusion of a wall effect in the minimum bed depth model. This is to be expected as the infinitesimal bed depth was set to balance the equation based on the provided desublimation energy duty. The infinitesimal bed depth would need to be justified in order to justify the energy balance.

For 18%, 8% and 4% CO₂ concentrations, the infinitesimal bed depth was set to 5 mm, 3 mm and 2 mm, respectively. The bed depths appear to align with the required bed depth to balance the heat transfer coefficient. A gas to solid heat transfer coefficient was calculated as part of the energy balance equation in Equation (14), and the heat transfer coefficient calculated is independent of the infinitesimal bed depth; however, the heat transfer coefficient can be calculated using the total heat transfer surface area of the infinitesimal bed depth. Comparisons of the two methods of heat transfer calculation are compared in Table 8.

Table 8. Comparison of different methods for calculation of heat transfer coefficient.

CO ₂ %	Heat Transfer Coefficient (Equation (16)) (W/m ² K)	Heat Transfer Coefficient from Minimum Bed Depth Model (W/m ² K)
18	177	191
8	193	191
4	193	190

The heat transfer coefficients calculated from two different methods were close to one another. Which gives confidence that the infinitesimal bed depth derived from iterative calculations to balance the minimum bed depth model is an accurate estimation. The heat transfer coefficient derived from the minimum bed depth utilises the overall temperature change of the solid bed from initial bed temperature to frosted bed temperature.

4.2. Larger Scale Simulation Comparison

The energy balance models were used to calculate the bed flow rate and energy duties for the direct gas cooled from Table 2. The results were then compared with the information provided in [10] to assess the validity of these energy balance models.

Tables 9 and 10 compare the results of the different mathematical models with the results simulated by Willson et al. [10] for the bed flow rate and the energy duty of the direct gas to bed heat exchanger. The mass flow balance model used was the adjusted Equation (18) where the applications involved temperature change discrepancies between the gas and solid phase, this primarily being the CCGT application.

Table 9. Comparison of volumetric bed flow rates (m^3/s) calculated by different energy balance models.

	Oil-Fired Boiler	CCGT	Biogas Upgrading
This work (Equation (12))	0.58	0.50	0.002
Minimum bed depth model (Equation (14))	0.58	0.50	0.002
Mass flow balance model (Equation (13))	0.58	0.50	0.002
Willson et al. [10]	0.55	0.19	0.002

Table 10. Comparison of energy duty of the desublimer calculated through different energy balance models.

	Oil-Fired Boiler (MW)	CCGT (MW)	Biogas Upgrading (kW)
This work (Equation (12))	20.1	6.4	84.0
Minimum bed depth model (Equation (14))	20.1	6.4	84.0
Mass flow balance model (Equation (13))	20.1	6.4	84.0
Willson et al. [10]	19.9	5.3	81.2

The moving bed calculations showed consistent results between the energy balance models with the energy duties and volumetric flow rates for the bed material stated in [10]. It is observed a discrepancy related to the CCGT case, the reason being due to the proposed energy balance models assuming temperature change for the bed material would rise from 154 K to the CO_2 desublimation temperature, which is related to CO_2 concentration and thus much lower for the CCGT case. For the oil-fired boiler and biogas upgrading examples, the CO_2 desublimation temperature was similar to or exceeded the initial gas temperature of 174 K, being 173 K for the oil-fired boiler and 183 K for the biogas upgrader, resulting in no difference between the two sets of calculated bed flow rates; however, for the CCGT example this assumption of bed material rising to the CO_2 desublimation temperature had a significant impact on the calculated bed flow rate as the desublimation temperature was approximately 161 K.

The bed flow rates and energy balance models overall appear to be fairly consistent at predicting the required energy duties of the solid and gas phases to maintain thermal equilibrium. The slightly modified version of available energy balance models was shown to predict moving bed behaviour with CO_2 desublimation. The methods presented with

similar results give confidence that cryogenic carbon capture with moving beds can be properly predicted using the described methods. In cases where the CO₂ gas mixture has an initial temperature equivalent to the CO₂ desublimation temperature, the mass flow balance model (13) provides accurate predictions for energy duty and required bed mass flow rate while requiring the fewest variables to calculate. For cases where the initial gas temperature is greater than the CO₂ desublimation temperature, the energy balance model proposed in (12) can effectively calculate mass flow rates and energy duties with a relatively simple method, whereas the infinitesimal bed depth model (14) requires an iterative process to estimate the required bed depth while being able to calculate additional aspects of moving bed heat exchange such as heat transfer coefficients. This work provides a clear method of designing a moving bed CCC process for specific applications where empirical evidence to support the design of moving beds may be lacking.

5. Conclusions

Three different proposed energy balance models for moving bed cryogenic CO₂ capture were evaluated using available experimental and simulated data for moving bed CCC processes. The proposed methods give consistent calculated bed flow rates when compared with each other and a high degree of accuracy with available simulated and experimental data, providing bed flow rate predictions of 0.026, 0.018 and 0.014 kg/s respectively for simulated gases with CO₂ % *v/v* concentration of 18%, 8% and 4% respectively when using any of the energy balances models developed in this study.

The simulated results for the experimental rig showed consistency with the experimental results. The energy duties required by the gas phase showed agreement among the three different methods and similarity with the energy duties calculated from experimental frost front velocities, with energy balance model energy duty predictions producing results with a proximity of 3.7%, 4.9% and 3.3% to experimentally derived results for CO₂ concentrations of 18%, 8% and 4%, respectively. The mass flow balance model showed a slight issue in predicting the required mass flow of bed material for moving bed cases where the temperature approach was assumed as negligible for the solid and gas phases, which is not always appropriate when including CO₂ desublimation within the model.

The simulated results from the energy balance models show good agreement with earlier simulated results, particularly in the oil-fired boiler and biogas upgrading cases. The developed energy balance models predicted energy duties with a proximity of 0.1%, 20.8% and 3.4% compared with the simulated results, respectively. Bed flow rate predictions matched up well with simulated results for the biogas upgrading and oil-fired boiler cases, with a matching prediction for the biogas upgrading case and a comparison of and a proximity of 5.5% for the oil-fired boiler. The calculated bed flow rate for the CCGT in the proposed models, however, did not accurately match the simulated results.

This work will benefit the design of cryogenic moving beds through effective simulation of MBHE energy balances with varying gas flow rates and compositions and moving bed sizes. This work also has potential applications for MBHEs beyond cryogenic applications to effectively simulate phase change of different gas purification systems such as wet gas drying. Further work to investigate the applicability of these energy models for potential wider applications should be performed before applying the models to such applications.

Author Contributions: D.C.: validation, formal analysis, investigation, writing—original draft, writing—review and editing. C.F.-P.: resources, writing—review and editing, visualization, supervision, project administration, Funding acquisition. All authors have read and agreed to the published version of the manuscript.

Funding: This research was funded by the Royal Academy of Engineering under the Leverhulme Trust Research Fellowship scheme (LTRF1920\16\18).

Acknowledgments: Carolina Font Palma thanks the fellowship supported by the Royal Academy of Engineering under the Leverhulme Trust Research Fellowship scheme.

Conflicts of Interest: The authors declare no conflict of interest.

Abbreviations

List of Nomenclature

a	surface area per unit volume m^2/m^3
A	Cross-sectional area m^2
B	Width of heat exchanger perpendicular to gas and solids flow m
c_p	specific heat capacity J/kgK
d	diameter m
D_{eff}	Effective diffusion coefficient
h	Heat transfer coefficient $\text{W}/\text{m}^2\text{K}$
H	Height of heat exchanger in solids flow direction m
dH	Infinitesimal bed depth m
Δh	Desublimation enthalpy J/mol
k	Thermal conductivity W/mK
L	Length of heat exchanger in gas flow direction m
m	mass kg
\dot{m}	mass flow rate kg/s
\dot{m}''	mass deposition rate per unit surface area $\text{kg}/\text{m}^2\text{s}$
n_c	number of components
Q	Energy duty W
dT	Change in temperature K
u	Velocity m/s
dz	bed depth

Greek Letters

ε	Bed voidage
λ_{eff}	Effective thermal conductivity
ω	mass fraction kg/kg
ρ	density kg/m^3

Subscripts and Superscripts

b	bed
g	gas
p	particle
s	solid
i	component i
w	wall

Appendix A

Gas phase compositions were input into REFPROP to retrieve gas phase characteristics; the desublimation temperature of the gas phase CO_2 mixture was used as the reference point in each example to retrieve values for the density and specific heat capacity of the gas.

Table A1. Simulated applications and calculated densities and specific heat capacities from REFPROP.

	Desublimation Temperature (K)	Density (kg/m^3)	Specific Heat Capacity (kJ/kgK)
Oil-fired boiler	173	2.141	982
CCGT	160.8	2.219	1009
Biogas upgrading	182.6	1.870	1292
Experimental rig 18% v/v CO_2	175.8	2.152	966
Experimental rig 8% v/v CO_2	168	2.124	1008
Experimental rig 4% v/v CO_2	162	2.167	1027

References

1. El-Sheikh, S. Conference of the Parties 2022, UNFCCC, Editor. 2022. Available online: <https://unfccc.int/documents/624444> (accessed on 24 November 2022).
2. Haszeldine, R.S. Carbon Capture and Storage: How Green Can Black Be? *Science* **2009**, *325*, 1647–1652. [CrossRef] [PubMed]

3. Font-Palma, C.; Cann, D.; Udemu, C. Review of Cryogenic Carbon Capture Innovations and Their Potential Applications. *C* **2021**, *7*, 58. [[CrossRef](#)]
4. Baxter, L.; Baxter, A.; Burt, S. Cryogenic CO₂ Capture as a Cost-Effective CO₂ Capture Process. In Proceedings of the 26th Annual International Pittsburgh Coal Conference 2009, PCC 2009, Pittsburgh, PA, USA, 20–23 September 2009; p. 1.
5. Song, C.-F.; Kitamura, Y.; Li, S.-H.; Jiang, W.-Z. Analysis of CO₂ frost formation properties in cryogenic capture process. *Int. J. Greenh. Gas Control* **2013**, *13*, 26–33. [[CrossRef](#)]
6. Jensen, M.J.; Russell, C.S.; Bergeson, D.; Hoeger, C.D.; Frankman, D.J.; Bence, C.S.; Baxter, L.L. Prediction and validation of external cooling loop cryogenic carbon capture (CCC-ECL) for full-scale coal-fired power plant retrofit. *Int. J. Greenh. Gas Control* **2015**, *42*, 200–212. [[CrossRef](#)]
7. Pan, X.; Clodic, D.; Toubassy, J. CO₂ capture by antisublimation process and its technical economic analysis. *Greenh. Gases Sci. Technol.* **2013**, *3*, 8–20. [[CrossRef](#)]
8. Tuinier, M.; Annaland, M.V.S.; Kramer, G.; Kuipers, J. Cryogenic CO₂ capture using dynamically operated packed beds. *Chem. Eng. Sci.* **2010**, *65*, 114–119. [[CrossRef](#)]
9. Tuinier, M.J.; van Sint Annaland, M.; Kuipers, J.A.M. A novel process for cryogenic CO₂ capture using dynamically operated packed beds—An experimental and numerical study. *Int. J. Greenh. Gas Control* **2011**, *5*, 694–701. [[CrossRef](#)]
10. Willson, P.; Lychnos, G.; Clements, A.; Michailos, S.; Font-Palma, C.; Diego, M.E.; Pourkashanian, M.; Howe, J. Evaluation of the performance and economic viability of a novel low temperature carbon capture process. *Int. J. Greenh. Gas Control* **2019**, *86*, 1–9. [[CrossRef](#)]
11. Cann, D.; Font-Palma, C.; Willson, P. Experimental analysis of CO₂ frost front behaviour in moving packed beds for cryogenic CO₂ capture. *Int. J. Greenh. Gas Control* **2021**, *107*, 103291. [[CrossRef](#)]
12. Cann, D.; Font-Palma, C.; Willson, P. Moving packed beds for cryogenic CO₂ capture: Analysis of packing material and bed precooling. *Carbon Capture Sci. Technol.* **2021**, *1*, 100017. [[CrossRef](#)]
13. Chen, Y.; Cann, D.; Jia, J.; Font-Palma, C. Preliminary study of CO₂ frost formation during cryogenic carbon capture using tomography analysis. *Fuel* **2022**, *328*, 125271. [[CrossRef](#)]
14. Johansson, M.T.; Söderström, M. Options for the Swedish steel industry—Energy efficiency measures and fuel conversion. *Energy* **2011**, *36*, 191–198. [[CrossRef](#)]
15. Saastamoinen, J.J. Comparison of Moving Bed Dryers of Solids Operating in Parallel and Counterflow Modes. *Dry. Technol.* **2005**, *23*, 1003–1025. [[CrossRef](#)]
16. Macias-Machín, A.; Cuéllar, J.; Estévez, A.; Jaraíz, E. Simple design of a crossflow moving bed heat exchanger-filter (MHEF). *Filtr. Sep.* **1992**, *29*, 155–161, 146. [[CrossRef](#)]
17. Henriquez, V.; Macias-Machin, A. Hot gas filtration, using a moving bed heat exchanger-filter (MHEF). *Chem. Eng. Process. Process Intensif.* **1997**, *36*, 353–361. [[CrossRef](#)]
18. Almendros-Ibáñez, J.; Soria-Verdugo, A.; Ruiz-Rivas, U.; Santana, D. Solid conduction effects and design criteria in moving bed heat exchangers. *Appl. Therm. Eng.* **2011**, *31*, 1200–1207. [[CrossRef](#)]
19. Hadley, T.D.; Pan, Y.; Lim, K.-S.; Orellana, J. Engineering design of direct contact counter current moving bed heat exchangers. *Int. J. Miner. Process.* **2015**, *142*, 91–100. [[CrossRef](#)]
20. Crawshaw, J.P.; Paterson, W.R.; Scott, D.M. Gas Channelling and Heat Transfer in Moving Beds of Spherical Particles. *Chem. Eng. Res. Des.* **2000**, *78*, 465–472. [[CrossRef](#)]

Disclaimer/Publisher’s Note: The statements, opinions and data contained in all publications are solely those of the individual author(s) and contributor(s) and not of MDPI and/or the editor(s). MDPI and/or the editor(s) disclaim responsibility for any injury to people or property resulting from any ideas, methods, instructions or products referred to in the content.